# Semi-Annual Status Report on NASA Grant NSG 1629

# "An Investigation of Vortex-Induced Aerodynamic Characteristics of Supersonic Cruise Configurations"

July 1, 1984 - December 31, 1984

by

C. Edward Lan

January 28, 1985

The Flight Research Laboratory

Department of Aerospace Engineering

The University of Kansas

Lawrence, Kansas 66045

The activities during this reporting period (July 1 - December 31, 1984) are described as follows.

(1) Nonlinear wave drag

The linear lifting-surface theory can predict reasonably well the lift in supersonic flow, but the drag is usually underpredicted. To remedy this deficiency, a simple method for calculating the nonlinear wave drag was developed. In the method, the calculated sectional drag is modified by adding the difference between the exact two-dimensional (2-D) and the linear 2-D wave drag at the calculated sectional lift coefficient. The results in most cases show good improvement in the supersonic drag prediction. All supersonic cases which were calculated previously were re-calculated. Two examples are presented in Figs. 1 and 2.

(2) Restructuring of the VORCAM code

At the suggestion of NASA users, the VORCAM code was modified for the Fortran 77 language. Its input stream was also rearranged. The work has been completed and has passed different tests so far. The only remaining task is the revision of user's manual.

(3) Boeing free-sheet code

Great effort and time have been spent in adapting the Boeing code to the computer system at KU. All CDC special features in the code have been replaced with standard Fortran algorithms. This was accomplished with the assistance of some CSC personnel at the Langley Research Center. At this time, the code has passed successfully through compilation. Currently,

execution test is under way.

(4) Investigation of asymmetric vortex separation

To account for the asymmetric vortex separation, additional vortex distribution on the wing is needed to satisfy the boundary condition. Since the present preliminary investigation is based on the Smith's code of slender wing theory, this additional vortex distribution was introduced in his transformed plane (Z*), instead of the physical plane (Z). In the transformed plane, the wing is a vertical slit as shown in Fig. 3. In a symmetrical vortex configuration, this additional vortex distribution should vanish.

Let $V(z^*)$ be the velocity induced on the transformed wing by the asymmetrical vortex system. To satisfy the boundary condition, a vortex distribution ($\gamma$) is introduced such that

$$\frac{1}{2\pi}\int_{-1}^{1}\frac{\gamma(z_1^*)\,dz_1^*}{z^*-z_1^*} = V(z^*) \tag{1}$$

Eq. (1) can be inverted to give

$$\gamma(z^*) = -\frac{2}{\pi}\sqrt{\frac{1-z^*}{1+z^*}}\int_{-1}^{1}\sqrt{\frac{1+\xi}{1-\xi}}\,\frac{V(\xi)}{z^*-\xi}\,d\xi + \frac{C}{\sqrt{(1-z^*)(1+z^*)}} \tag{2}$$

In the thin airfoil theory, C is always zero because of Kutta condition. In the present case, the leading edge is at $y^* = 0$ and $z^* = 0$. It follows that $\gamma(0) = 0$. Hence

$$C = \frac{2}{\pi}\int_{-1}^{1}\sqrt{\frac{1+\xi}{1-\xi}}\,\frac{V(\xi)}{-\xi}\,d\xi \tag{3}$$

To integrate Eq. (2), let

$$z^* = -\cos\theta$$
$$\xi = -\cos\theta' \tag{4}$$

To evaluate the two integrals in Eq.(2), note that

$$I_1 = \int_{-1}^{1} \sqrt{\frac{1+\xi}{1-\xi}}\, \frac{V(\xi)}{z^*-\xi}\, d\xi = \int_0^{\pi} \frac{1-\cos\theta'}{\cos\theta'-\cos\theta} V(\theta')\, d\theta' \tag{5}$$

$$I_2 = \int_{-1}^{1} \sqrt{\frac{1+\xi}{1-\xi}}\, \frac{V(\xi)}{\xi}\, d\xi = \int_0^{\pi} \frac{1-\cos\theta'}{-\cos\theta'} V(\theta')\, d\theta' \tag{6}$$

Now, if

$$V(\theta')(1-\cos\theta') = A_0 + \sum_1^{\infty} A_n \cos n\theta', \tag{7}$$

then

$$A_n = \frac{2}{\pi} \int_0^{\pi} V(\theta')(1-\cos\theta')\cos n\theta'\, d\theta', \quad n \neq 0,$$
$$A_0 = \frac{1}{\pi} \int_0^{\pi} V(\theta')(1-\cos\theta')\, d\theta' \tag{8}$$

Therefore,

$$I_1 = \sum_1^{\infty} A_n \pi \frac{\sin n\theta}{\sin\theta} \tag{9}$$

$$I_2 = -\sum_1^{\infty} A_n \pi \sin n\frac{\pi}{2} \tag{10}$$

Using Eqs. (9) and (10), Eq. (2) can be rewritten as

$$\gamma(z^*) = -\frac{2}{1+z^*}\sum_{1}^{\infty} A_n \sin n\theta + \frac{2}{\sqrt{(1-z^*)(1+z^*)}}\sum_{1}^{\infty} A_n \sin n\frac{\pi}{2} \quad (11)$$

Using the above formulation, it is expected that if the asymmetrical vortex system can be predicted by an inviscid method, the additional vortex distribution in Fig. 3 would play an important role. So far, several ideas have been tested with the revised code. The vortex cores are always moved in a direction to minimize the force based on a combined gradient and conjugate gradient method.

a) Movement of vortex cores.

It is found that to have a better convergence characteristics one vortex core should be moved first than the other, instead of moving both at the same time.

b) Step sizes

Instead of having the same step size for $y_v^*$ and $z_v^*$, it is preferred to have separate step sizes in some cases.

c) Updating of wing boundary condition

Updating of wing boundary condition represents another level in the iterative method of solutions. It is not apparent when and how often the wing boundary condition should be updated. In the revised code, option is provided to update the wing boundary condition either at the beginning only or as often as practical.

d) Convergence criteria

The most difficult condition to be satisfied is the force free condition for the vortex and its cut. Instead of specifying a small error as a convergence criterion, it is preferred to start with a larger error and decrease it gradually. The results of any run, whether converged or not, are always kept on disk files for subsequent possible rerun.

Some preliminary results are described below. Note that the starting asymmetrical vortex shapes are generated from the symmetrical shapes at different angles of attack. The results in Fig. 4 are for a $\theta_{max}$ of 200 deg. (an angle through which a sheet turns around the core). It is seen that the resulting shapes, though not as asymmetrical as expected, are not symmetrical either. The configuration is further compared with the symmetrical case in Fig. 5. Another indicator of asymmetry is the vortex distribution ($\gamma$). Fig. 6 shows the $\gamma$-distribution. Note that $\gamma$ is referenced to $U \cot \Lambda_{LE}$ .

At the suggestion of Dr. Dick Barnwell of NASA Langley, $\theta_{max}$ is increased to 450 deg. so that the vortex sheet will wrap around the core further. In this case, if the starting shapes on both sides are too much different, the force-free condition on the vortex sheets to determine the strengths is frequently violated and the calculation will just stop. Therefore, the starting shapes are generated corresponding to a = 8 and 6 respectively. Note that for $\alpha$ = 25 deg., a = 7.134. The resulting shapes after reaching an average vortex force equal to $\varepsilon_z = 10^{-4}$ are compared in Fig. 7 and the additional vortex distribution ($\gamma$) is shown

in Fig. 8. Note that large $\gamma$ near $z^* = \pm 1$ implies large tangenial velocity near the center of the physical wing. A tuft-grid survey of the flow field for this wing is presented in Fig. 9. Unfortunately, the survey was made at a station behind the wing trailing edge, instead of over the wing.

A main conclusion from this study is that perhaps because of nonlinearity, the solution appears to be nonunique. One possible mechanism of vortex asymmetry has been "crowding" of two vortices. This is being investigated at the present time.

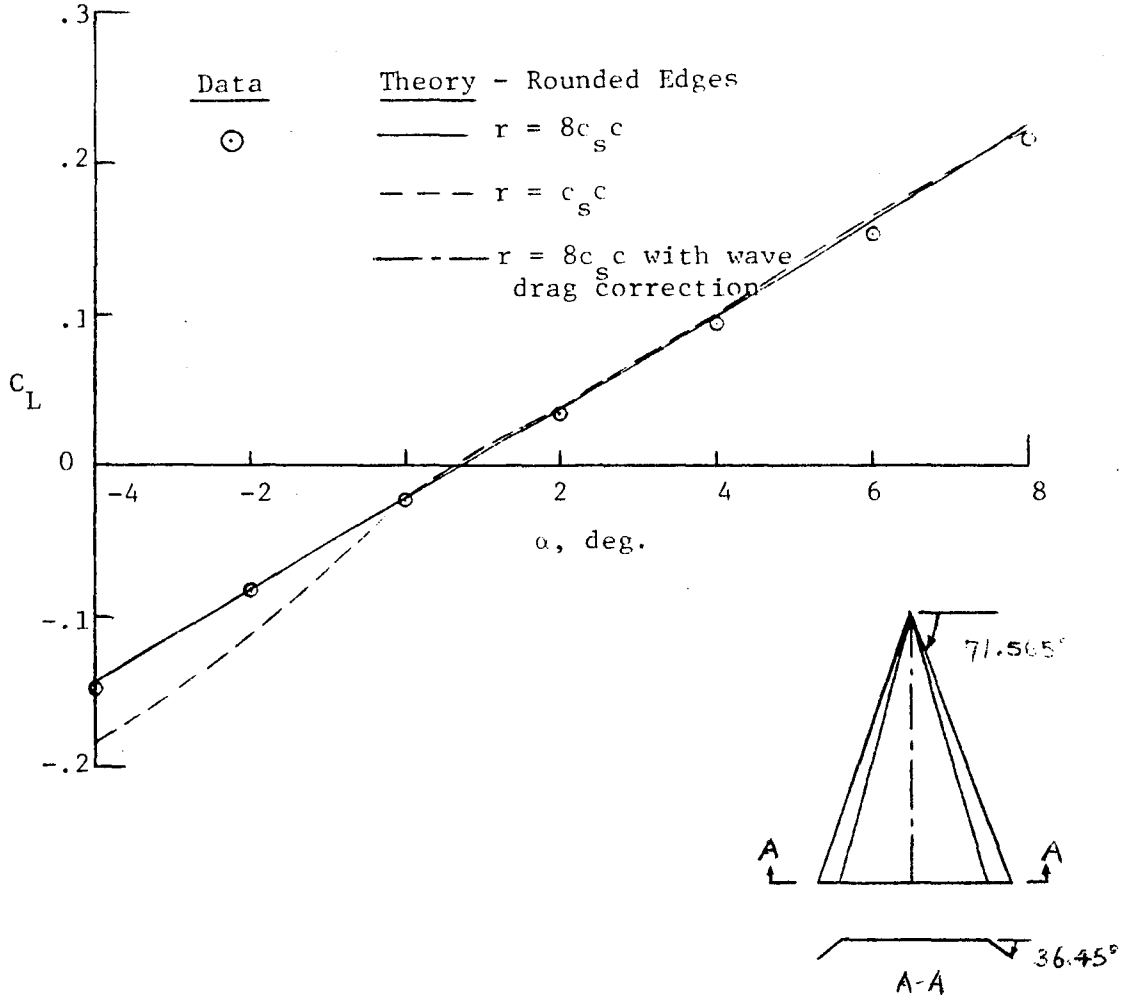


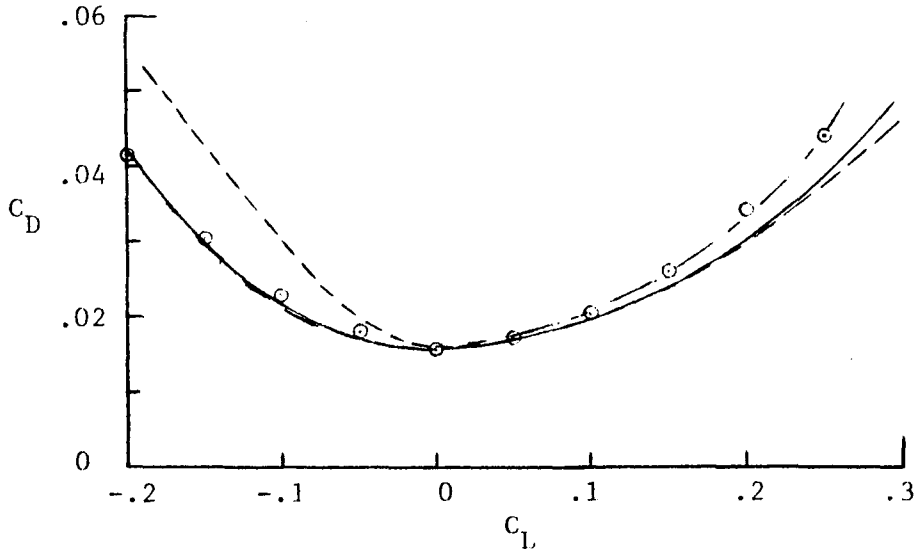


Figure 1 Aerodynamic Characteristics of a Wing Alone at M =1.8

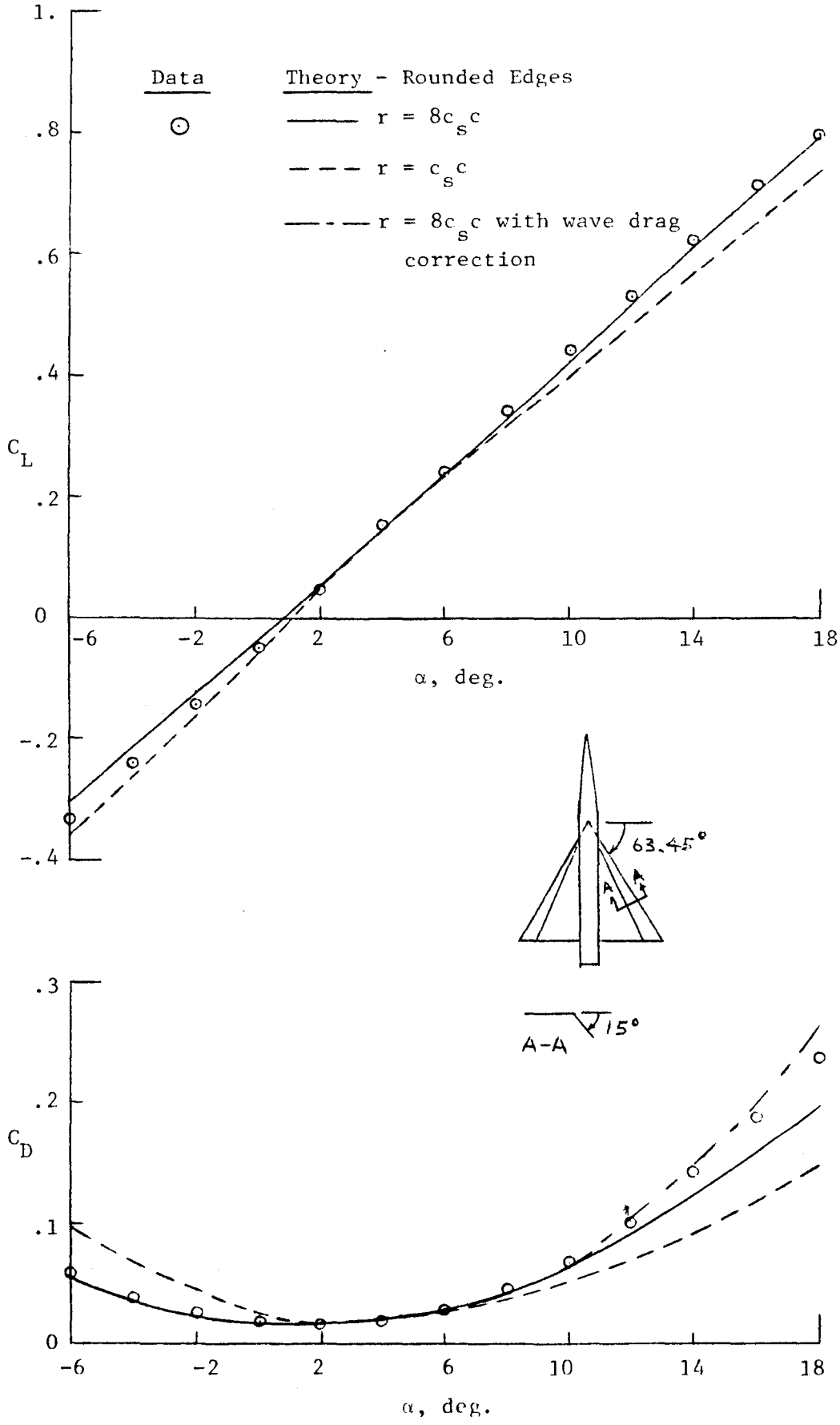


Figure 2 Aerodynamic Characteristics of a Wing-Body Combination at M = 1.3.

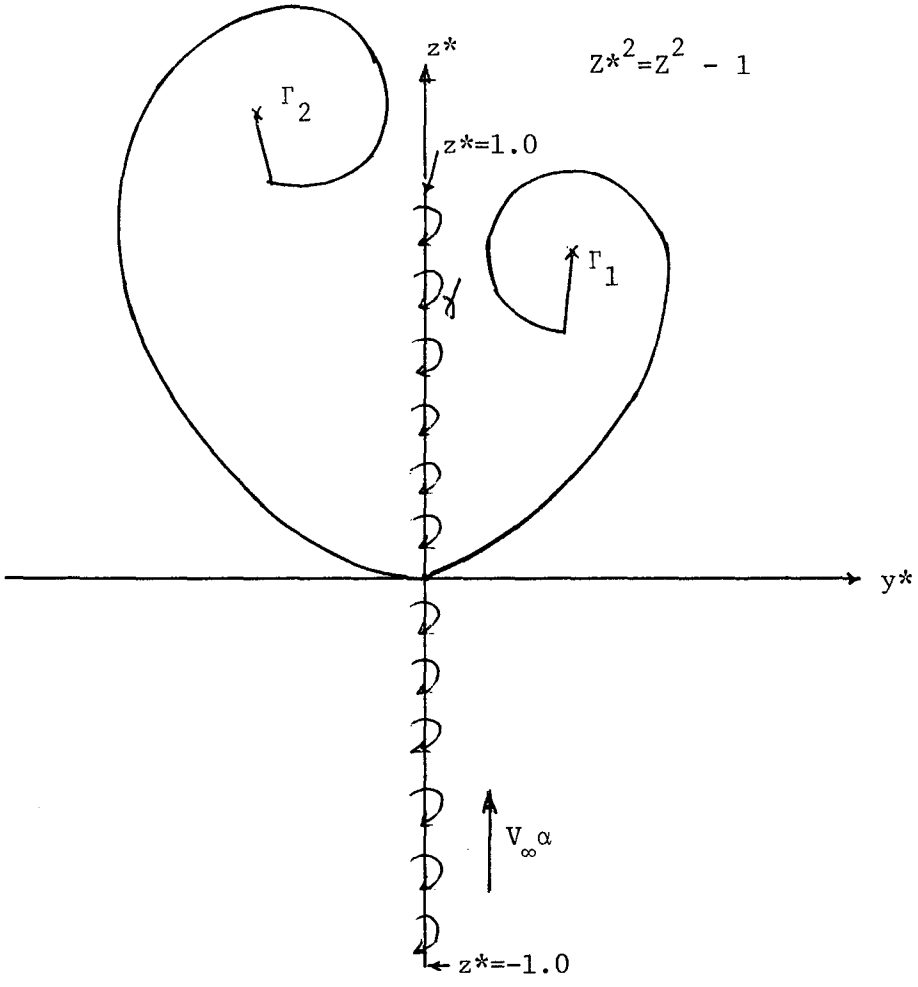


Figure 3 Possible Asymmetrical Vortex System on the Transformed Plane

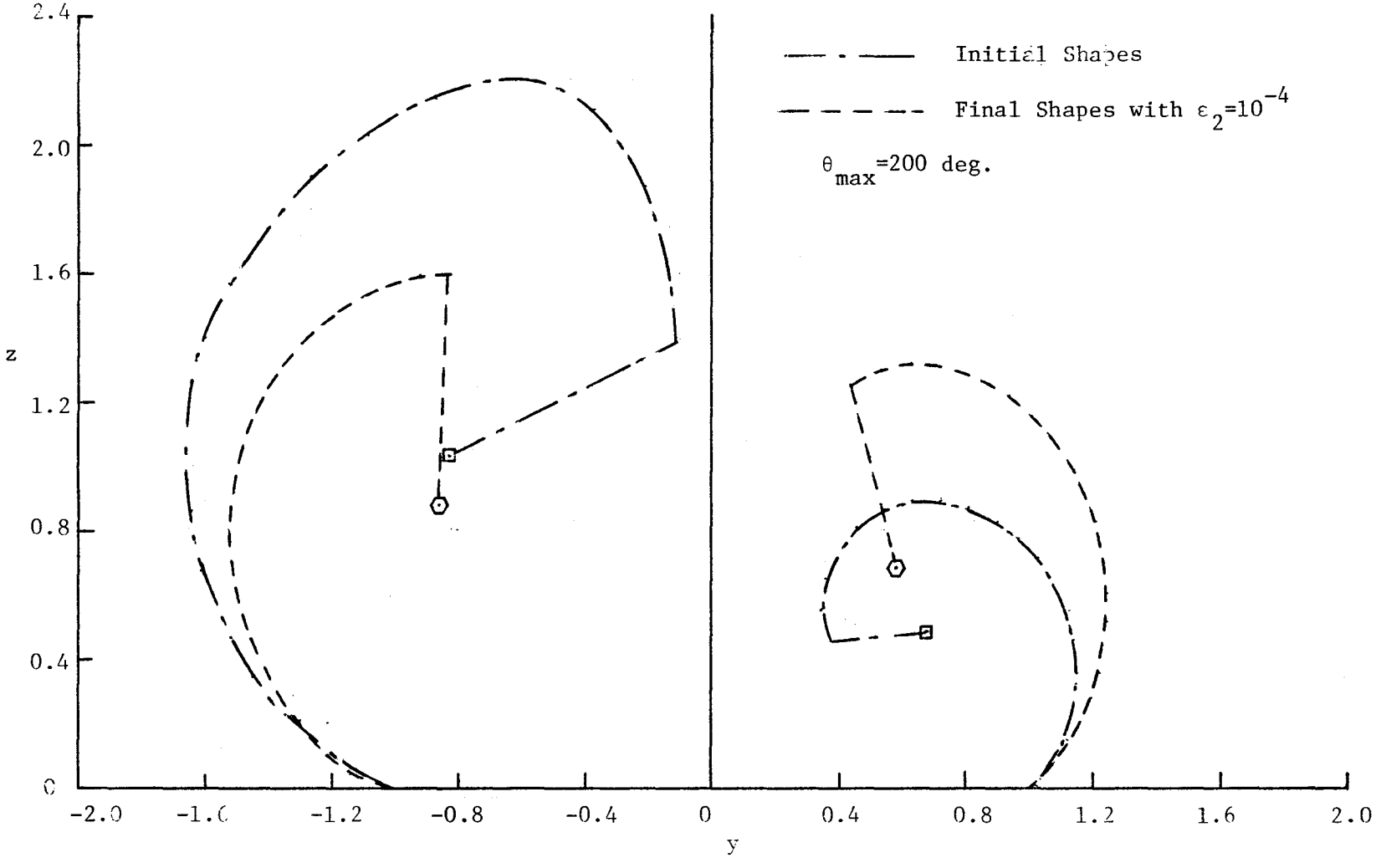


Figure 4 Vortex Shapes for 86.5-deg Delta Wing at $\alpha$ = 25 deg.

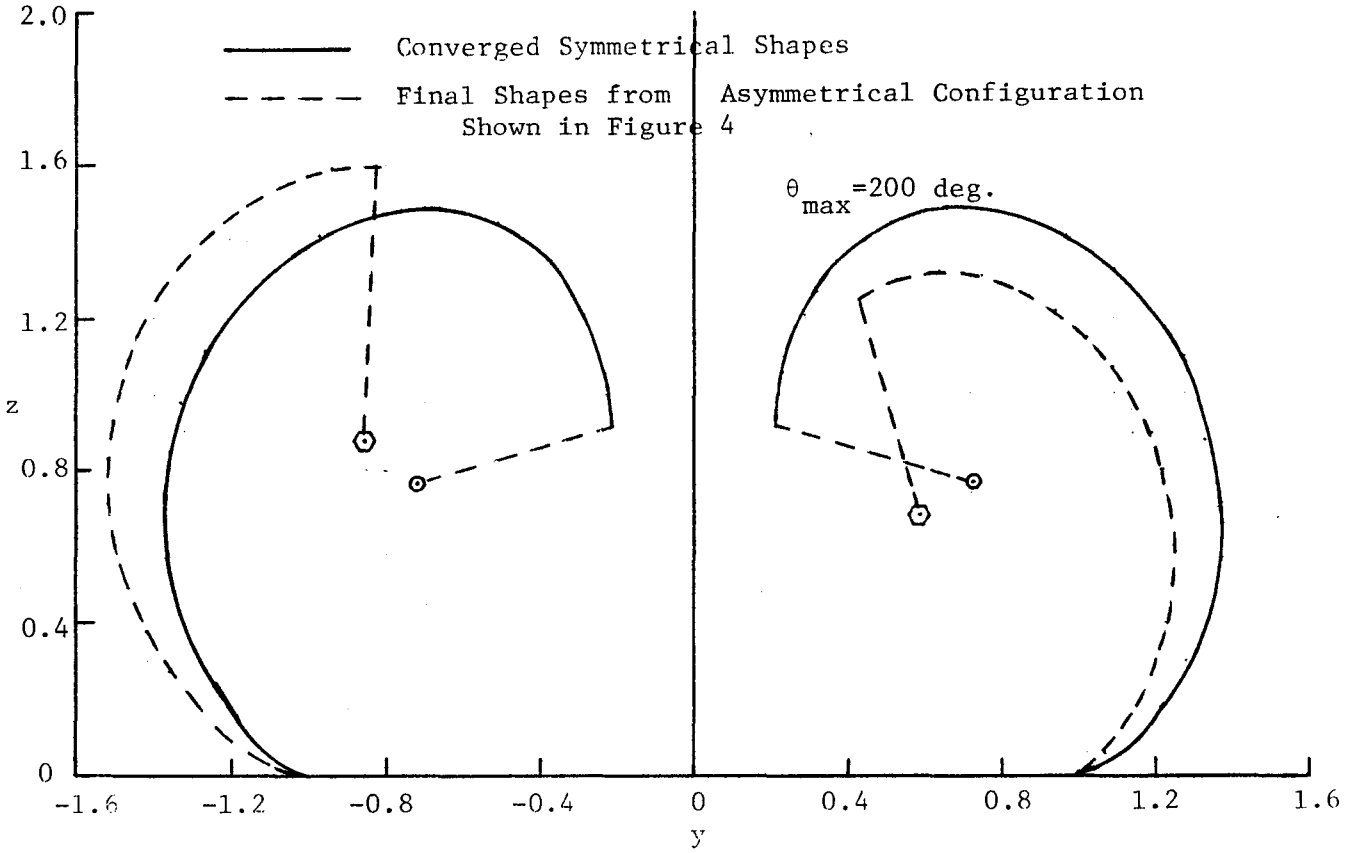


Figure 5 Vortex Shapes for 86.5-deg. Delta Wing at $\alpha$ = 25 deg.

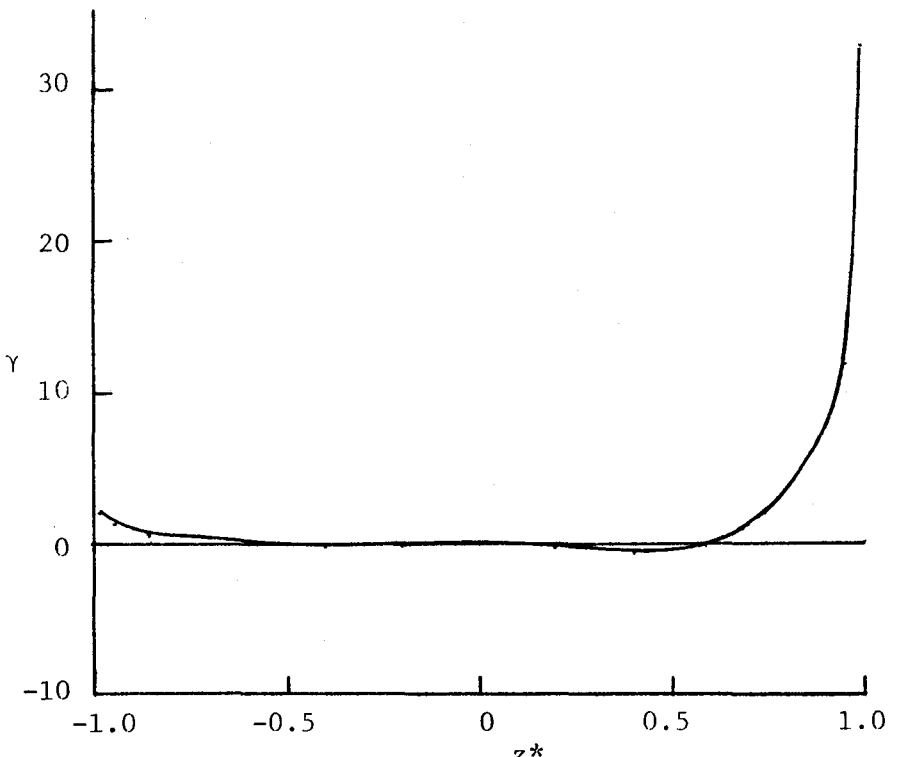


Figure 6 Additional Vortex Distribution on the Wing due to Vortex Asymmetry

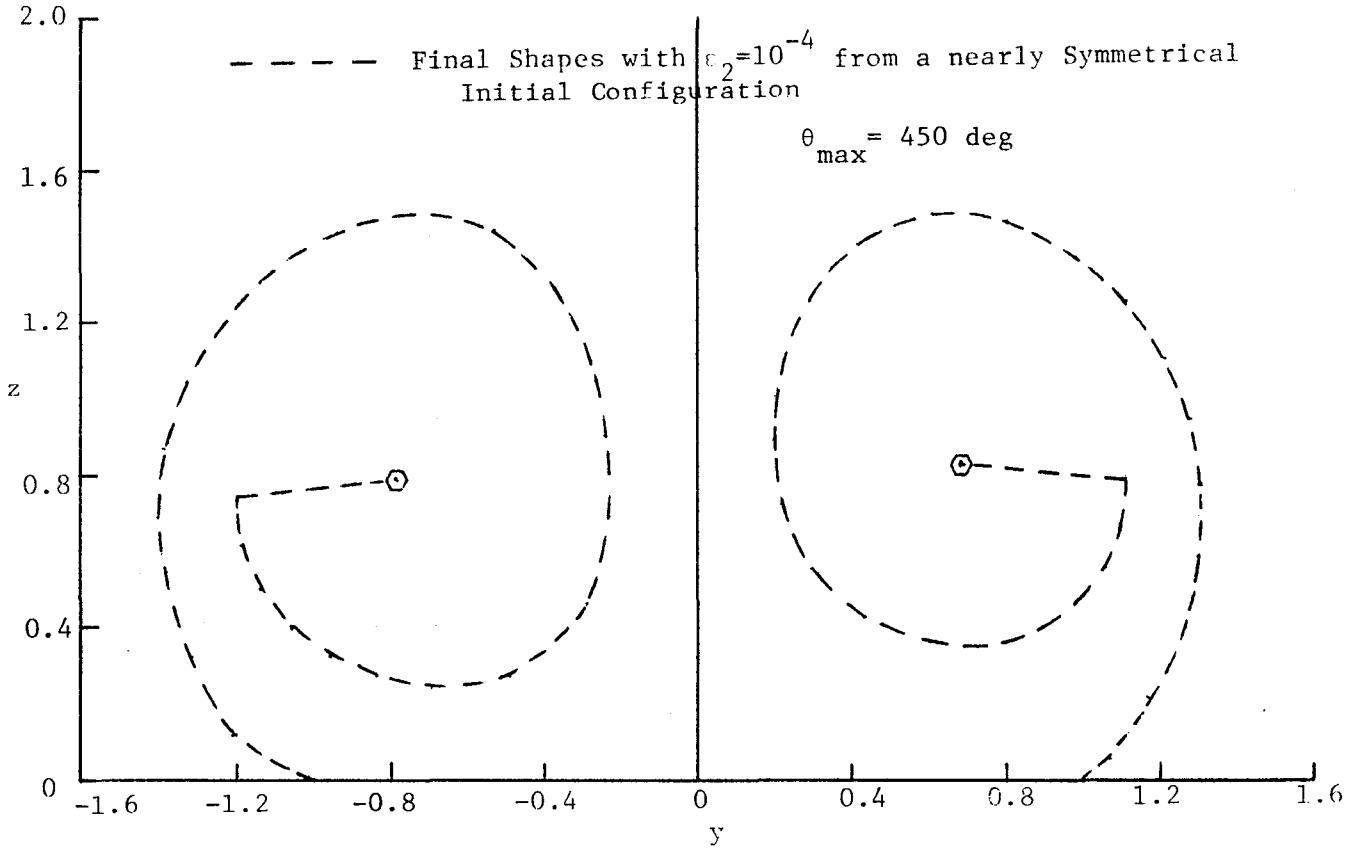


Figure 7 A Possible Vortex System for 86.5-deg Delta Wing at $\alpha$ = 25 deg

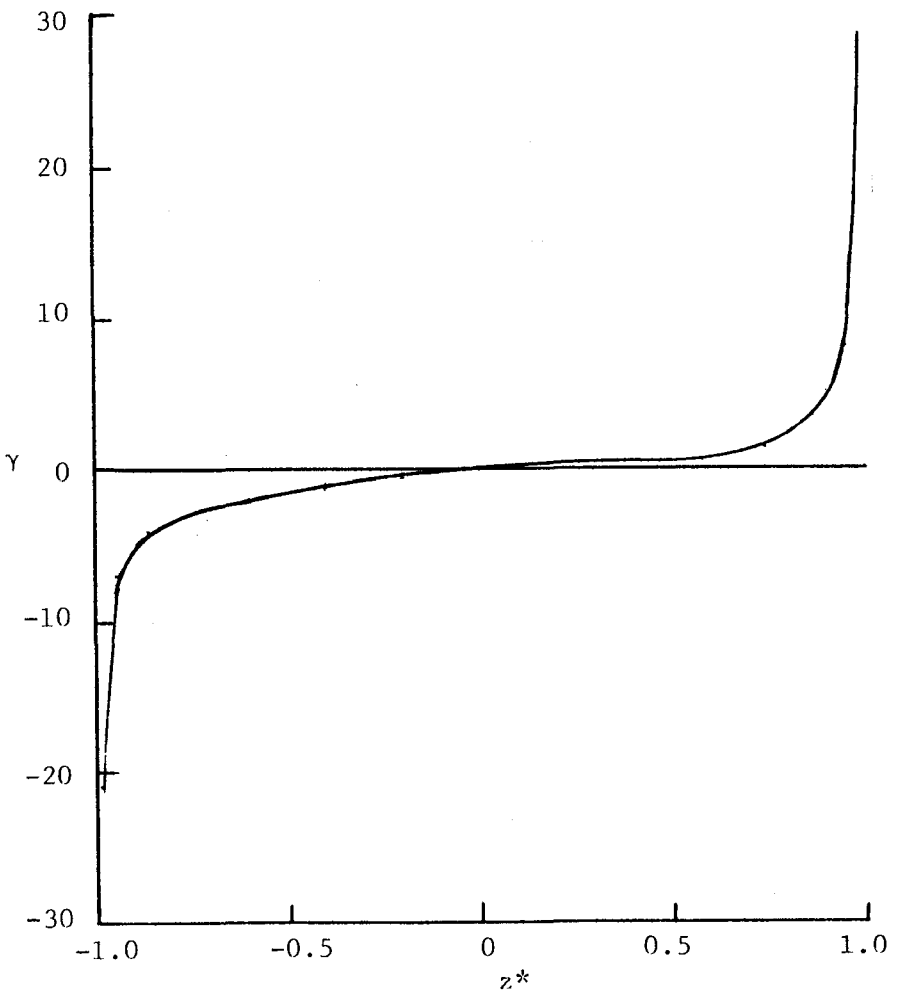


Figure 8 Additional Vortex Distribution on the Wing due to Vortex Asymmetry

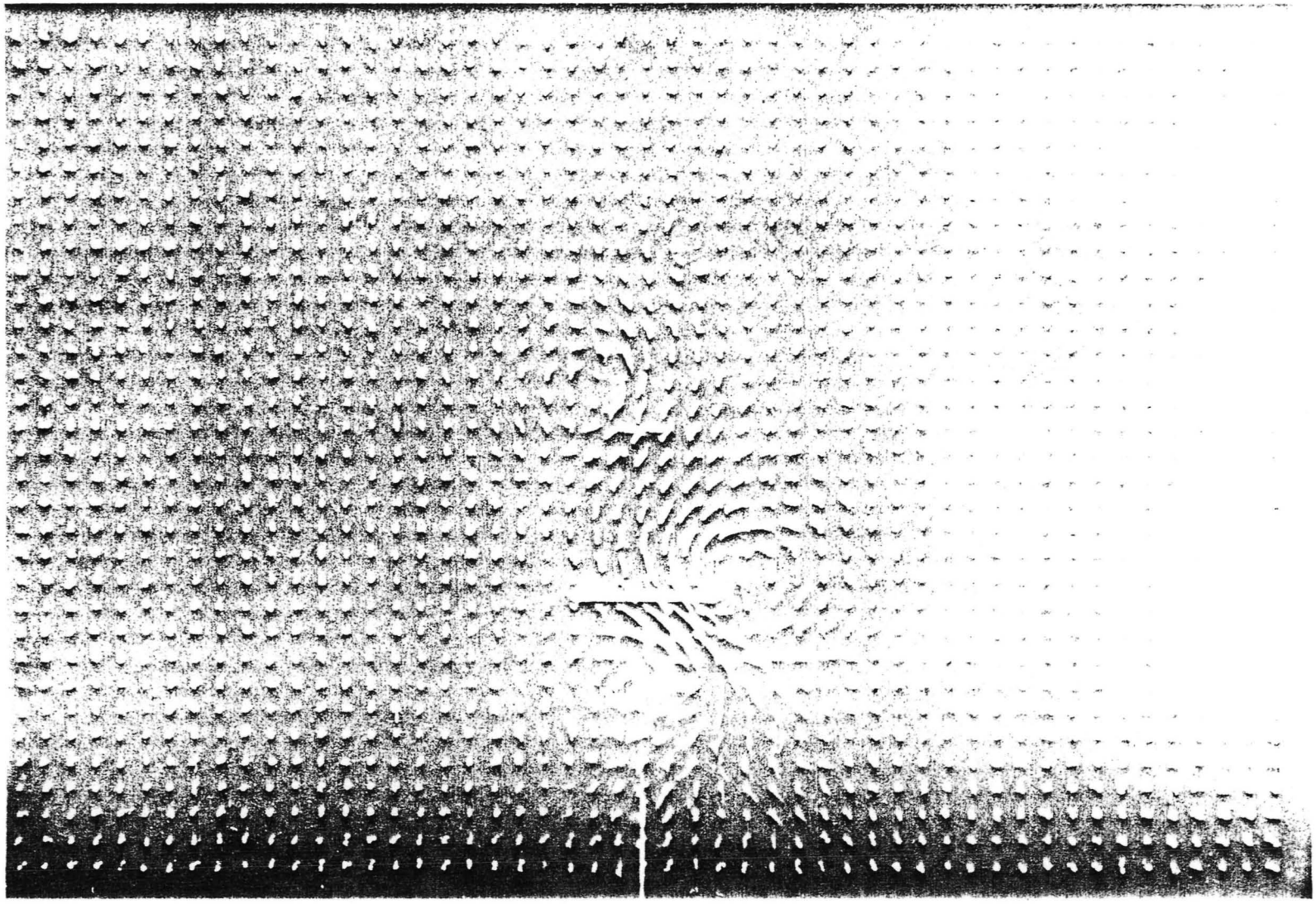

L-68-10,056

Figure 9 A tuft-grid survey at about $0.2c_r$ behind the trailing edge of a flat-plate delta wing with an $86.5^0$ sweep of the leading edges for $\alpha = 25^0$ and $\beta = 0^0$.

NASA TN D-5045